Journal of Human Genetics (2017) 62, 531–537

www.nature.com/jhg

ORIGINAL ARTICLE

Cryptic splice activation but not exon skipping is observed in minigene assays of dystrophin c.9361+1G>A mutation identified by NGS

Emma Tabe Eko Niba[1], Atsushi Nishida[1], Van Khanh Tran[2], Dung Chi Vu[3], Masaaki Matsumoto[4], Hiroyuki Awano[4], Tomoko Lee[5], Yasuhiro Takeshima[5], Hisahide Nishio[6] and Masafumi Matsuo[1]

Next-generation sequencing (NGS) discloses nucleotide changes in the genome. Mutations at splicing regulatory elements are expected to cause splicing errors, such as exon skipping, cryptic splice site activation, partial exon loss or intron retention. In dystrophinopathy patients, prediction of splicing outcomes is essential to determine the phenotype: either severe Duchenne or mild Becker muscular dystrophy, based on the reading frame rule. In a Vietnamese patient, NGS identified a c.9361+1G>A mutation in the dystrophin gene and an additional DNA variation of A>G at +117 bases in intron 64. To ascertain the consequences of these DNA changes on dystrophin splicing, minigene constructs were prepared inserting dystrophin exon 64 plus various lengths of intron 64. Exon 64 skipping was observed in the minigene construct with 160 nucleotide (nt) of intron 64 sequence with both c.9361+1A and +117G. In contrast, minigene constructs with larger flanking intronic domains resulted in cryptic splice site activation rather than exon skipping. Meanwhile, the cryptic splice site activation was induced even in +117G when intron 64 was elongated to 272 nt and longer. It was expected that cryptic splice site activation is an *in vivo* splicing outcome.
Journal of Human Genetics (2017) **62,** 531–537; doi:10.1038/jhg.2016.162; published online 19 January 2017

INTRODUCTION

Dystrophinopathies such as Duchenne or Becker muscular dystrophy (DMD/BMD) are one of the most common inherited muscular diseases and are caused by mutations in the dystrophin gene. The gene spans >2 400 kb on the X chromosome and encodes a 14-kb complementary DNA (cDNA) consisting of 79 exons. Nearly two-thirds of the identified mutations in the dystrophin gene are deletions/duplications of one or more exons. The remaining one-third of patients may be affected by heterogeneous small mutations, including point mutations.[1,2] The clinical application of next-generation sequencing (NGS) as a diagnostic tool has become increasingly evident.[3–5] Likewise, mutations in the dystrophin gene have been disclosed using NGS.[6–9]

DMD is a fatal progressive muscle-wasting disease, with patients succumbing in the second or third decades of life, whereas BMD is an adult onset slowly progressive muscle-wasting disease. The differences between severe DMD and mild BMD can be explained by the reading frame rule, namely that mutations disrupting the reading frame of the dystrophin mRNA result in severe DMD, whereas those maintaining the reading frame result in mild BMD.[10] This reading frame rule is applicable to more than 90% of dystrophinopathy patients. Therefore, it is essential to determine the reading frame of aberrant dystrophin mRNA to predict the clinical phenotype of dystrophinopathy, especially in splice site mutations.

Regulation of the splicing of dystrophin pre-mRNA is considered to be extraordinarily sophisticated because the dystrophin gene contains seven alternative promoters, huge introns[11] and 14 cryptic exons.[12] Furthermore, activation of cryptic splice sites in dystrophin introns has been reported in cultured human cells as well.[13,14] Splicing errors of dystrophin pre-mRNA have been identified in mutations at not only the consensus sequences for splice sites, but also at those for splicing regulatory elements.[2,15–17]

There is still no established method for predicting how such mutations will affect pre-mRNA splicing.[18,19] It has been reported that the majority of splicing errors caused by mutations at donor sites comprised exon skipping, whereas cryptic splice site usage was predominant at acceptor sites.[19–22] Minigene splicing assays have been employed to disclose the pathogenicity of nucleotide changes.[23,24] In dystrophinopathy, splicing outcome of splice site mutation has been investigated by minigene splicing assay.[25,26] For mutations at the first nucleotide of a dystrophin intron (+1G), two patterns of splicing outcomes, exon skipping

[1]Department of Physical Therapy, Faculty of Rehabilitation, Kobe Gakuin University, Kobe, Japan; [2]Center for Gene and Protein Research, Hanoi Medical University, Hanoi, Vietnam; [3]Department of Medical Genetics, Metabolism and Endocrinology and Clinical Research, Research Institute for Child Health, Vietnam National Hospital of Pediatrics, Hanoi, Vietnam; [4]Department of Pediatrics, Kobe University Graduate School of Medicine, Kobe, Japan; [5]Department of Pediatrics, Hyogo College of Medicine, Japan and [6]Department of Community Medicine and Social Healthcare Science, Kobe University Graduate School of Medicine, Kobe, Japan
Correspondence: Professor M Matsuo, Department of Physical Therapy, Faculty of Rehabilitation, Kobe Gakuin University, 518 Arise, Ikawadani, Nishi, Kobe 6512180, Japan.
E-mail: mmatsuo@reha.kobegakuin.ac.jp
Received 20 May 2016; revised 1 December 2016; accepted 7 December 2016; published online 19 January 2017

and cryptic splice site activation, have been identified, with exon skipping being the most common (www.dmd.nl).[27] In our previous study, it was hypothesized that cryptic splice site activation by +1G mutations occurs in the exons with high exon recognition strength.[27]

In the present study, NGS disclosed a nucleotide change of c.9361+1G>A in a Vietnamese patient. The splicing outcomes of the +1G>A mutation accompanying +117A>G in dystrophin intron 64 were analyzed by minigene splicing assays. The cryptic splice site activation was expected to occur in *in vivo* splicing. The index case was supposed to result in BMD.

MATERIALS AND METHODS

Patient

The index patient was an 11-year-old Vietnamese boy. He started independent walking at 2 years. At 5 years, he showed signs of muscle weakness. He exhibited a positive Gowers' sign as well as pseudohypertrophy, and his serum creatine kinase was 14 355 IU l^{-1} (normal: <300 IU l^{-1}). He was clinically diagnosed as dystrophinopathy and referred to the National Hospital of Pediatrics, Hanoi, Vietnam, for genetic diagnosis. As the first step, the deletion/duplication of the 79 dystrophin exons was examined by a standard method of multiplex ligation probe amplification.[6] However, no abnormalities were identified in the amplified products (data not shown).

Ion torrent semiconductor sequencing

Targeted sequencing was performed using the Ion Torrent Platform (Life Technologies, Carlsbad, CA, USA) in accordance with the manufacturer's specifications, as described previously.[6] Briefly, an AmpliSeq Library Kit 2.0 (Life Technologies) was used together with an AmpliSeq IDP (Life Technologies) that targets 300 gene-encoding proteins related to more than 700 inherited diseases. Filtered variants were annotated using both Ion Reporter Software v4.6 (Life Technologies) and Ingenuity Variant Analysis Software (Qiagen, Hilden, Germany), and the alignments were visualized using Integrative Genomics Viewer (IGV v.2.1; Broad Institute, Cambridge, MA, USA).

In vitro splicing analysis

In vitro splicing assays were conducted using the preconstructed minigene expression vector H492 encoding two exons (A and B) and a multicloning site for insertion of a test sequence consisting of an exon and its flanking introns.[28] The region encompassing exon 64 (157 nucleotides (nt) of the 3′ end of intron 63, 75 bp of exon 64 and various lengths of intron 64 ranging from 160 to 1196 nt) was polymerase chain reaction (PCR)-amplified from the genomic DNA of the index case, a normal control subject and a Japanese patient with the identical splice site mutation but no single-nucleotide change at the 117th nt of intron 64 (manuscript in preparation). For the Japanese patient, informed consent was obtained at Kobe University Hospital, and the study was approved by the Kobe University Ethical Committee. Five different lengths of intron 64 (160, 272, 404, 680 and 1196 nt) were PCR-amplified using different primer sets (one common forward primer and five different reverse primers; Supplementary Table 1). The products were then digested with restriction enzymes *Nhe*I and *Bam*HI (New England Biolabs, Ipswich, MA, USA) and inserted into the H492 vector predigested with the same enzymes. All minigenes were sequenced to confirm their structures.

For splicing assays, the minigenes were transfected into HeLa cells obtained from ATCC (Manassas, VA, USA). The transfected cells were harvested after 24 h and their total RNA was extracted using a High Pure RNA Isolation Kit (Roche Diagnostics, Basel, Switzerland). The extracted RNA was quantified using a NanoDrop 2000 spectrophotometer (Thermo Fisher Scientific, Waltham, MA, USA). An amount corresponding to 500 ng of total RNA was used for cDNA synthesis with M-MLV Reverse Transcriptase (Invitrogen, Carlsbad, CA, USA), RNaseOut Recombinant Ribonuclease Inhibitor (Invitrogen), Random Hexamers (Invitrogen) and dNTP mixture (TaKaRa Bio, Shiga, Japan) in a total volume of 20 μl as described previously.[29] For examination of the splicing products, the T7 promoter forward and bGH reverse primers (Supplementary Table 1) were used for PCR. PCR amplifications were carried out using the conditions described in our previous report.[27] The integrity and concentration of the cDNA were examined by amplifying the mRNA of a housekeeping gene, *glyceraldehyde 3-phosphate dehydrogenase* (*GAPDH*), using reverse transcriptase PCR (RT-PCR) for 18 cycles using a specific primer set (Supplementary Table 1).

The RT-PCR-amplified products were separated and semi-quantified using a DNA 1000 LabChip Kit and a 2100 Bioanalyzer (both from Agilent Technologies, Santa Clara, CA, USA).

DNA sequencing

For confirmation of the mutation, the patient's genomic DNA was extracted from a peripheral blood sample, and the exon 64-encompassing region was PCR-amplified using a specific primer set (Supplementary Table 1) under previously described conditions.[29] The PCR product was directly sequenced. For analysis of minigene splicing products, the RT-PCR products were sequenced after subcloning into the pT7 blue T vector (Novagen, San Diego, CA, USA). Sequencing was conducted by Greiner Bio-One (Tokyo, Japan).

Splice site strength and splicing motif analysis

The splice site strength and splicing motifs were analyzed using Human Splicing Finder (www.umd.be/HSF3/) as described previously.[30] The splicing probability score was determined through the same website using the algorithm of Yeo and Burge.[31]

RESULTS

For the index case, the mutation in the dystrophin gene was identified by targeted NGS. The pile-up data obtained by the targeted NGS showed that the 31241164th nt was T in the dystrophin gene of the patient, whereas it was C in the normal control subject (Figure 1a). This finding indicated a nucleotide change from C to T, corresponding to a G-to-A change at the first nt of intron 64. Accordingly, Sanger sequencing of the exon 64-encompassing genomic region confirmed an A nucleotide at the first nt (+1) of dystrophin intron 64 (c.9361+1G>A; Figure 1b). Unexpectedly, an additional single-nucleotide change was identified at the 117th nt of intron 64, replacing A with G (c.9361+117A>G; Figure 1c). c.9361+117G was considered to be a novel single-nucleotide polymorphism in intron 64, and was not found in the Japanese patient with the identical c.9361+1G>A mutation (Figure 1c). Accordingly, the two nucleotide changes were not present in the control subject (Figure 1c).

The mutation of c.9361+1G>A disrupted the conserved GT dinucleotides at the splice donor site and decreased the splice site consensus value from 82.62 to an un-nominated level. Skipping of exon 64 was supposed to occur with this mutation because mutations at +1G in the dystrophin gene were reported to commonly induce upstream exon skipping.[27] Although this supposition could be examined by analysis of dystrophin mRNA expressed in the skeletal muscle of the patient, a muscle biopsy sample of the index case was not available owing to a limitation of the medical facilities in Vietnam.

Instead, the consequences of c.9361+1G>A were examined by minigene-based *in vitro* splicing assays. The exon 64-encompassing region including 160 nt of intron 64 was PCR-amplified and inserted into the H492 vector. The constructed minigenes were subjected to splicing in HeLa cells and the resultant mRNAs were RT-PCR-amplified. From the normal minigene (DI64.160wA), one amplified product containing exons A, 64, and

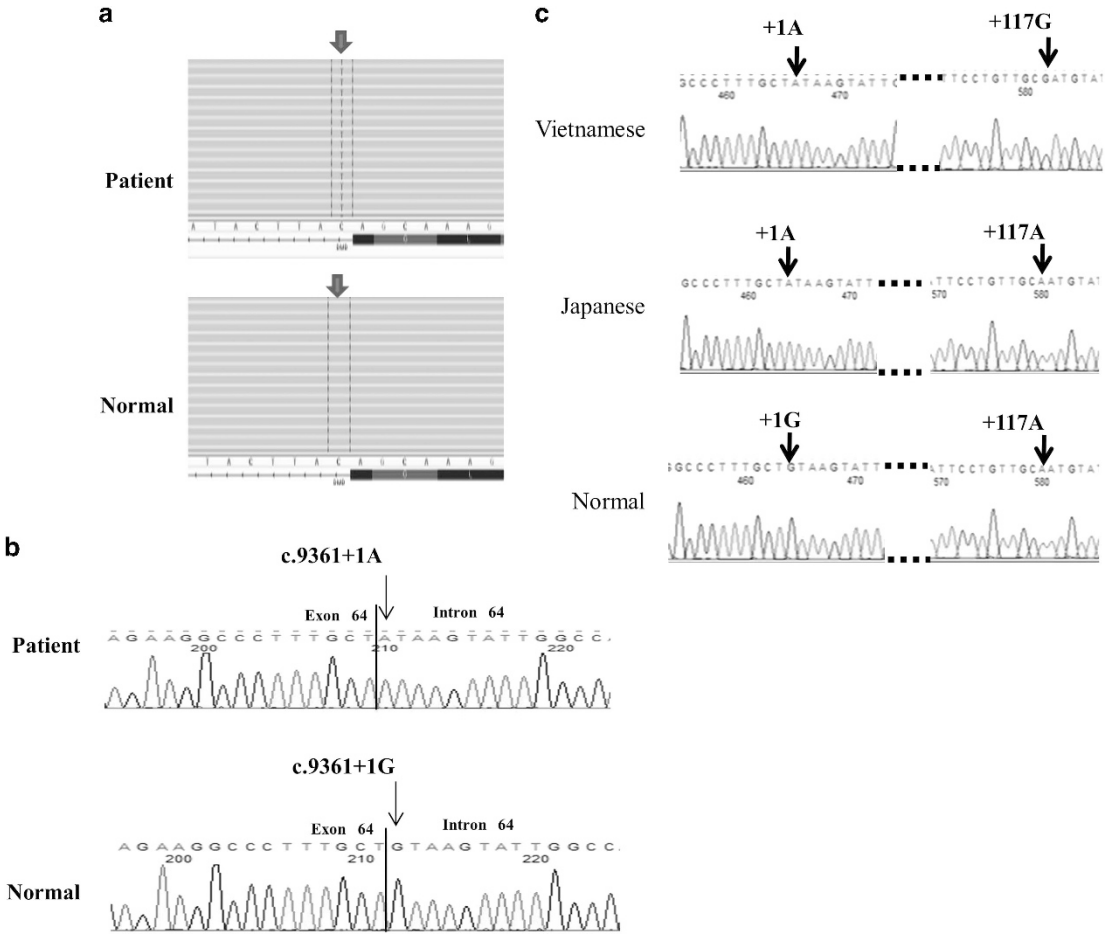

Figure 1 Nucleotide changes within intron 64. (**a**) Read pile-up data obtained from the Ion Personal Genome Machine (PGM). The read pile-up data of the boundary between exon 64 and intron 64 of the dystrophin gene are shown. In the index case, only T was detected at the 31 241 164th nucleotide (nt; nucleotide number on X chromosome from Human Genome Resources at ncbi.nlm.nih.gov; upper arrow), while only C was detected in the normal control subject (lower arrow). This nucleotide change corresponded to a G-to-A transition at the first nucleotide of intron 64 of the dystrophin gene (c.9361+1G>A). (**b**) Sequence of the junction between exon 64 and intron 64. Sanger sequencing of the exon 64-encompassing region was conducted. A part of the sequence of the boundary between exon 64 and intron 64 is shown. At the first nucleotide of intron 64, an A nucleotide was identified in the index case (upper), whereas G was identified in the normal control subject (lower). The nucleotide change corresponded to c.9361+1G>A. (**c**) Sequences around the 1st and 117th nt of intron 64. A part of the exon 64 and intron 64 sequence obtained by Sanger sequencing is shown. The index case had both A at the 1st nt and G at the 117th nt in intron 64 (upper), whereas the normal control subject had G and A at both the 1st and 117th nt (lower), respectively. A Japanese patient with c.9361+1A had A at the 117th nt (middle). A full color version of this figure is available at the *Journal of Human Genetics* journal online.

B was obtained, showing the normal splicing process (Figure 2a). However, a smaller product was obtained from the minigene with two mutations of c.9361+1A and +117G (DI64.160mG; Figure 2a). Sequencing of the product revealed the absence of exon 64 from the mature mRNA, indicating exon 64 skipping. This strongly suggested that exon 64 skipping is the splicing outcome caused by c.9361+1G>A, as expected. As exon 64 encodes 75 nt, the exon 64-skipped mRNA was considered to maintain an ability to produce dystrophin deleting 25 amino acids.

As DI64.160mG contained the additional mutation of +117G, another minigene replacing this mutation with A (DI64.160 mA) was constructed and subjected to splicing. Unexpectedly, this minigene produced a larger-size band (Figure 2a). Sequencing of the product revealed a 57-nt insertion between exons 64 and B. The inserted 57 nt completely matched with the 5′ end sequence of intron 64, indicating retention of intron 64. Examination of the genomic sequence of intron 64 showed that GT dinucleotides, known as the splice donor site consensus sequence, were present at the 58th and 59th nt of intron 64 (Figure 2b). The consensus value for the donor splice site was calculated at 80.13, implying a cryptic splice site, whereas the consensus value for the authentic non-mutated site was 82.62. Therefore, it was concluded that the cryptic splice site was activated in DI64.160 mA. Contrary to the previous result, the cryptic splice site activation was suggested to occur with c.9361+1G>A.

The above results showed that the splicing outcome of the +1G>A mutation was influenced by the nucleotide composition at the 117th position. In other words, the +117G mutation completely hampered usage of the cryptic splice donor site, whereas +117A allowed recognition of the site. The nucleotide at the 117th position was suggested to have a critical role in the recognition of the cryptic splice site. Therefore, the sequences around the 117th nt were examined for splicing motifs using Human Splicing Finder. The results revealed the presence of a splicing silencer.[32] In the case of the wild-type +117A, the splicing silencer strength of tgttgcaa (underline indicates A at the 117th position) was 64.64, whereas

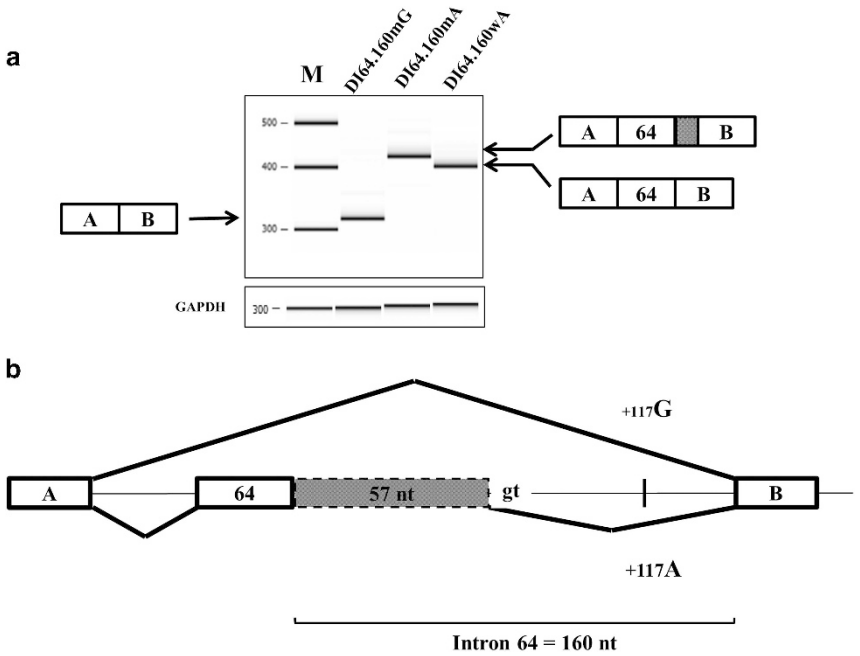

Figure 2 Splicing analysis of minigenes with 160 nucleotides (nts) of intron 64. (**a**) Reverse transcription polymerase chain reaction (RT-PCR) products of the minigene transcripts. Minigenes with 160-nt intron 64 were subjected to splicing and the resulting mRNAs were analyzed by RT-PCR amplification. Electrophoregrams of the RT-PCR-amplified products are shown. Minigenes carrying the normal sequence (c.9361+1G and +117A; DI64.160wA), mutated sequence from the Vietnamese patient (c.9361+1G>A and +117G; DI64.160mG) and mutated sequence from the Japanese patient (c.9361+1G>A and +117A; DI64.160mA) produced one clear band with differing sizes. Sequencing of each product was conducted. The normal sequence (DI64.160wA) produced a mature mRNA consisting of exons A, 64 and B. Meanwhile, DI64.160mG produced a small-size product with complete exon 64 skipping. In contrast, DI64.160mA produced a large-size product with insertion of a 57-nt intron 64 sequence between exons 64 and B. M refers to the size markers. The identities of the splicing products are indicated on either side. The boxes and numbers within the boxes indicate the exons and exon numbers, respectively. The shaded box indicates the 57-nt intron 64 insertion. GAPDH mRNA was amplified to observe the amount of material (below). (**b**) Schematic representation of the splicing of the minigenes with 160-nt intron 64. The boxes and bars indicate the exons and introns, respectively. The numbers in the boxes refer to the exon number. The shaded box represents the inserted intron sequence (57 nt). A GT dinucleotide was identified downstream of the 3′ end of the inserted sequence. The upper and lower diagonal lines indicate splicing of +117G and +117A, respectively.

the splicing silencer strength of the mutant +117G (ttgttgcga) increased to 75.30. It was indicated that the +117G suppressed the usage of the cryptic splice site as a splicing silencer.

Although a striking difference in the splicing outcomes caused by a single-nucleotide change at the +117th nt was observed in minigenes with 160 nt of intron 64, it was of concern that this length of intron 64 was too short to simulate *in vivo* splicing. Therefore, the length of the added intron 64 was elongated to 272 nt in the respective minigenes (DI64.272wA, DI64.272mA and DI64.272mG). For the normal minigene (DI64.272wA), one product consisting of exons A, 64 and B was obtained. In contrast, two mutant minigenes encoding c.9361+1G>A and +117A (DI64.272mA) or +117G (DI64.272mG) produced the same size product (Figure 3). The product was confirmed to have a 57-nt insertion between exons 64 and B. In DI64.272 mA, a fairly visible band was revealed (Figure 3a). Sequencing of this product revealed a 4-nt insertion between exons 64 and B. Other GT dinucleotides conserved at donor splice site were identified at the 5th and 6th nt (Figure 3c). However, the donor site consensus value was very low. This result indicated that another cryptic splice site was activated at a very low level.

Remarkably, we obtained different splicing products from two mutant minigenes encoding different sizes of intron 64. It was postulated that the splicing silencer activity of +117G for the cryptic splice site was blocked by elongation of intron 64 (DI64.272mG). Therefore, the elongated sequence from 161 to 272 nt was anticipated to contain a splicing enhancer for the cryptic splice site. Thus, the sequence from 161 and 272 nt of intron 64 was examined for a splicing motif. Remarkably, the sequence of agatat (underline indicates the difference from the consensus sequence) extending from the 228th to 233rd nt was found to be highly homologous to the consensus hexamer for an intronic splicing enhancer (aggtat).[33] Therefore, this sequence was indicated to activate the cryptic splice site usage.

The cryptic splice site usage was found to be influenced by two separate intronic elements. It was suggested that another motif would be present at a distant position. Thus, intron 64 was elongated to 404 nt in minigenes, and the splicing products were analyzed (Figure 3b). The splicing products obtained from the three minigenes matched those of the respective minigenes with 272-nt intron 64. Different from the minigenes with 272-nt intron 64, both DI64.404mG and DI64.404mA exhibited a fairly visible product with a 4-nt insertion (Figure 3b). Furthermore, minigenes with longer lengths of intron 64 (680 and 1196 nt) were prepared and subjected to *in vitro* splicing (Figure 4). However, the result of splicing of intron 64 presented similar results to that of figure 3, except that there was no product with insertion of 4-nt intron 64 (data not shown). These findings indicated that no more splicing regulatory elements with significant effects on the cryptic splice site usage were present in the downstream region of intron 64. Taking all of the above

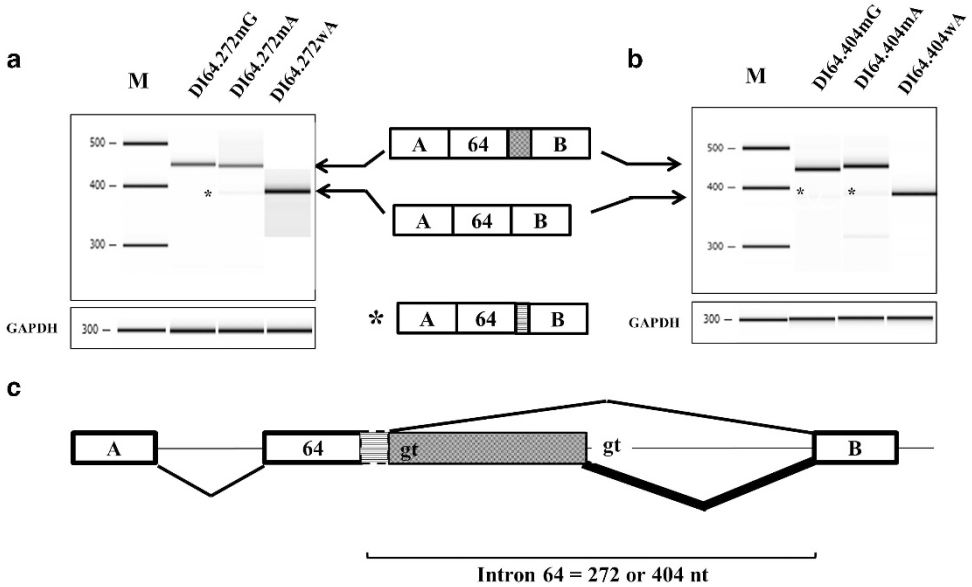

Figure 3 Splicing analysis of the minigenes with 272 and 404 nucleotide (nt) of intron 64. (**a**) Reverse transcription polymerase chain reaction (RT-PCR) products of the transcripts from the minigenes with 272-nt intron 64. Minigenes with 272-nt intron 64 were subjected to splicing, and the resulting mRNAs were analyzed by RT-PCR amplification. Electrophoregrams of the RT-PCR-amplified products are shown. Minigenes carrying the normal sequence (c.9361+1G and +117A; DI64.272wA), mutated sequence of c.9361+1G>A and +117A>G (DI64.272mG) and mutated sequence of c.9361+1G>A and +117A (DI64.272mA) produced one clear band. The sequence of each product revealed that the normal sequence produced a mature mRNA consisting of exons A, 64 and B. Both DI64.272mG and DI64.272mA produced a large-size product with insertion of the 57-nt intron 64 sequence between exons 64 and B. In addition, DI64.272mA revealed a very weak band (asterisk). The identities of the splicing products are indicated on the right. The boxes and numbers within the boxes indicate the exons and exon numbers, respectively. GAPDH mRNA was amplified to observe the amount of material (below). (**b**) RT-PCR products of the minigene transcripts with 404-nt intron 64. Minigenes with 404-nt intron 64 were subjected to splicing, and the resulting mRNAs were analyzed by RT-PCR amplification. Electropherograms of the RT-PCR-amplified products are shown. The three minigenes produced one clear band as described in **a**. Both DI64.404mG and DI64.404mA produced a tiny amount of product with 4-nt intron 64 insertion (asterisks). GAPDH mRNA was amplified to observe the level of material (below). (**c**) Schematic representation of the splicing of the minigenes with 272 and 404 nt of intron 64. Trace amounts of 4-nt intron 64 insertion were revealed in DI64.272mA, DI64.404mG and DI64.404mA. GT dinucleotides were presented at 5 and 6th nt of intron 64. The upper and lower diagonal lines indicate splicing of the cryptic splice sites at the 5th and 58th nt of intron 64, respectively. The bold diagonal lines indicate the major splicing pathway.

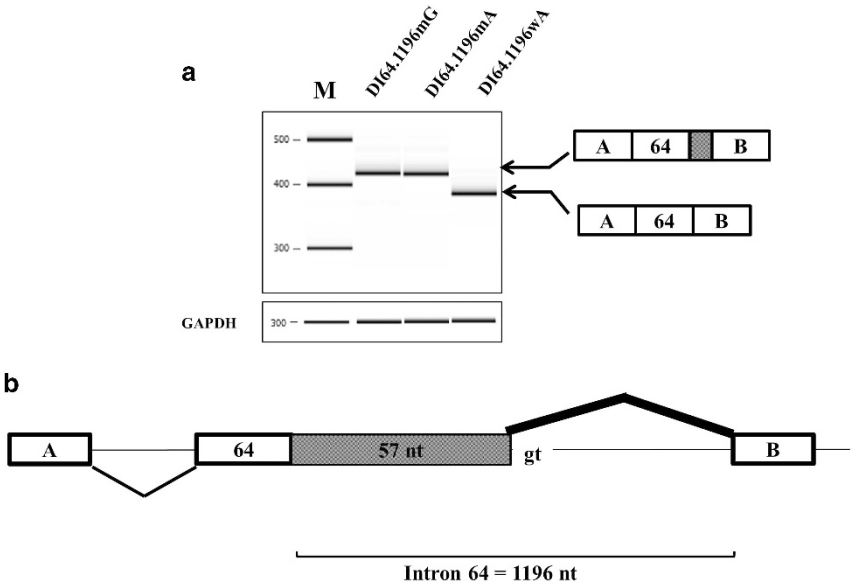

Figure 4 Splicing analysis of minigenes with 1196 nt of intron 64. (**a**) Minigenes with 1196-nt intron 64 were subjected to splicing and the resulting mRNAs were analyzed by RT-PCR amplification. Electrophoregrams of the RT-PCR-amplified products are shown. The three minigenes produced one clear band. The two mutant minigenes produced 57-nt intron 64-retaining transcripts in common (DI64.1196mG and DI64.1196mA), while the normal sequence produced a mature transcript (DI64.1196wA). (**b**) Schematic representation of the splicing of the minigenes with 1196 nt of intron 64. The diagonal line indicates splicing of the cryptic splice site.

results together, it was indicated that cryptic splice site activation is the splicing outcome of the index case.

DISCUSSION

In the present study, the NGS-based strategy successfully identified a single-nucleotide mutation of c.9361+1G>A at the 5′ end of intron 64 of the dystrophin gene in a Vietnamese patient (Figure 1). The identical nucleotide change was previously reported once in a dystrophinopathy case showing the clinical phenotype of an intermediate between DMD and BMD.[34] However, the splicing outcome that arose from the mutation remained unclear because no information on the dystrophin mRNA was available for this case.[34] Our case was the second to have the c.9361+1G>A mutation, but complicated with an additional nucleotide change at the 117th nt of intron 64 (Figure 1). Therefore, determination of the splicing outcomes of the double mutations was conducted by minigene splicing assays. When the downstream intron size was short, exon 64 skipping was observed (Figure 2). In contrast, cryptic splice site activation was observed in the presence of the wild-type +117A. This dramatic splicing change was suggested to arise through an increase in the splicing silencer strength provided by the A-to-G change. In the same way, single-nucleotide changes in deep introns have been shown to affect splicing.[35,36] In the era of NGS, it is an indication that even a single-nucleotide change in a deep intron should be taken into account when explaining splicing outcomes.

Among the 78 dystrophin introns, 50 have been reported to be mutated at +1G (www.dmd.nl). The most common mutation was a G-to-A change.[37] Even among these +1G>A mutations, the splicing outcomes differed from intron to intron. The most remarkable findings were obtained for c.4518 +1G>A and G>C in intron 32, which produced two splicing products with cryptic splice site activation in both exon and intron.[38] Therefore, it appears very difficult to establish a rule that can predict splicing outcomes. It has been proposed that exon skipping is the preferred pathway when the immediate vicinity of the affected exon–intron junction is devoid of alternative cryptic splice sites.[20] However, it has remained under discussion why a potentially high cryptic splice site is not always activated by splice site mutations. Our results indicated that cryptic splice site activation requires other elements. Previously, we reported that the availability of a cryptic splice site is not a determinant for splicing pathways of intron +1G>A mutations in the dystrophin gene, and proposed a hypothesis that strong exon recognition through the combination of a high splice acceptor site score and a long exon length is a determining factor for splicing pathways.[27] However, exon 64 was defined as a strong exon and should be skipped according to this definition.[27] This again indicates the difficulties associated with predicting splicing outcomes caused by mutations.

The splicing regulation of the dystrophin pre-mRNA has been attracting much attention because induction of exon skipping with an antisense oligonucleotide is the most promising therapy for DMD.[39–41] This establishment of exon-skipping therapy was initiated by the identification of exon skipping caused by a small intraexonic deletion consisting of an exonic splicing enhancer in a DMD patient.[22,40–42] Our results showed that a single-nucleotide change was able to induce dramatic changes in splicing (Figure 2). More efforts are required to further understand the splicing regulation toward the establishment of DMD treatments.

It was remarkable that the cryptic splice activation became the splicing pathway when the intron size was elongated to 272 nt or longer (Figures 3 and 4). The splicing results of the minigenes with elongated intron 64 were considered to simulate *in vivo* splicing, and it was conceived that cryptic splice site activation was the splicing outcome in the index case. This activation created a novel dystrophin mRNA retaining 57-nt-long intron 64 between exons 64 and 65. The retained 57 nt of intron 64 maintained the original dystrophin reading frame. It was supposed that dystrophin with additional 19 amino acids and two amino-acid changes encoded at the junction between the exon and intron is produced in the patient. The insertion of 19 amino acids was within the dystroglycan-binding domain of dystrophin and exerted devastating damage to dystrophin function, resulting in a severe DMD phenotype. However, the 57-nt intron 64 retention observed in the 5th nt mutation (c.9361+5G>C)[43] has been identified in BMD. In our case, the retained 57-bp sequence harbored no stop codon, implying that the translational machinery was not disturbed. Therefore, there is a possibility that some dystrophin is produced in our case as well rendering the phenotype milder. The patient was supposed to show a mild phenotype, but it is necessary to follow up long term to conclude this.

CONFLICT OF INTEREST

MM is an advisor for JCR Pharma, Japan and Daiichi Sankyo, Japan. The remaining authors declare no conflict of interest.

ACKNOWLEDGEMENTS

This work was supported by Japan Society for the Promotion of Science Grants-in-Aid for Scientific Research (KAKENHI; 24390267 and 26860803), a Research Grant for Research on Psychiatric and Neurological Diseases and Mental Health from Japan Agency for Medical Research and Development, AMED, and an Intramural Research Grant for Neurological and Psychiatric Disorders from the National Center of Neurology and Psychiatry (NCNP). We are grateful for technical assistance from Mina Murakami.

ETHICAL STANDARDS

The mutation study was approved by ethical committees of National Hospital of Pediatrics, Kobe University and Kobe Gakuin University and the mutation analysis of the dystrophin gene was carried out after obtaining informed consent from the parents of the patient.

1 Aartsma-Rus, A., Van Deutekom, J. C., Fokkema, I. F., Van Ommen, G. J. & Den Dunnen, J. T. Entries in the Leiden Duchenne muscular dystrophy mutation database: an overview of mutation types and paradoxical cases that confirm the reading-frame rule. *Muscle Nerve* **34**, 135–144 (2006).
2 Takeshima, Y., Yagi, M., Okizuka, Y., Awano, H., Zhang, Z., Yamauchi, Y. *et al.* Mutation spectrum of the dystrophin gene in 442 Duchenne/Becker muscular dystrophy cases from one Japanese referral center. *J. Hum. Genet.* **55**, 379–388 (2010).
3 Rehm, H. L. Disease-targeted sequencing: a cornerstone in the clinic. *Nat. Rev. Genet.* **14**, 295–300 (2013).
4 Sikkema-Raddatz, B., Johansson, L. F., de Boer, E. N., Almomani, R., Boven, L. G., van den Berg, M. P. *et al.* Targeted next-generation sequencing can replace Sanger sequencing in clinical diagnostics. *Hum. Mutat.* **34**, 1035–1042 (2013).
5 Valencia, C. A., Ankala, A., Rhodenizer, D., Bhide, S., Littlejohn, M. R., Keong, L. M. *et al.* Comprehensive mutation analysis for congenital muscular dystrophy: a clinical PCR-based enrichment and next-generation sequencing panel. *PLoS ONE* **8**, e53083 (2013).
6 Niba, E. T., Tran, V. K., Tuan-Pham, L. A., Vu, D. C., Nguyen, N. K., Ta, V. T. *et al.* Validation of ambiguous MLPA results by targeted next-generation sequencing discloses a nonsense mutation in the DMD gene. *Clin. Chim. Acta* **436**, 155–159 (2014).
7 Roucher Boulez, F., Menassa, R., Streichenberger, N., Manel, V., Mallet-Motak, D., Morel, Y. *et al.* A splicing mutation in the DMD gene detected by next-generation sequencing and confirmed by mRNA and protein analysis. *Clin. Chim. Acta* **448**, 146–149 (2015).
8 Taniguchi-Ikeda, M., Takeshima, Y., Lee, T., Nishiyama, M., Awano, H., Yagi, M. *et al.* Next-generation sequencing discloses a nonsense mutation in the dystrophin gene from long preserved dried umbilical cord and low-level somatic mosaicism in the proband mother. *J. Hum. Genet.* **61**, 351–355 (2016).

9 Okubo, M., Minami, N., Goto, K., Goto, Y., Noguchi, S., Mitsuhashi, S. *et al.* Genetic diagnosis of Duchenne/Becker muscular dystrophy using next-generation sequencing: validation analysis of DMD mutations. *J. Hum. Genet.* **61**, 483–489 (2016).
10 Monaco, A. P., Bertelson, C. J., Liechti-Gallati, S., Moser, H. & Kunkel, L. M. An explanation for the phenotypic differences between patients bearing partial deletions of the DMD locus. *Genomics* **2**, 90–95 (1988).
11 Ahn, A. H. & Kunkel, L. M. The structural and functional diversity of dystrophin. *Nat. Genet.* **3**, 283–291 (1993).
12 Zhang, Z., Habara, Y., Nishiyama, A., Oyazato, Y., Yagi, M., Takeshima, Y. *et al.* Identification of seven novel cryptic exons embedded in the dystrophin gene and characterization of 14 cryptic dystrophin exons. *J. Hum. Genet.* **52**, 607–617 (2007).
13 Nishida, A., Minegishi, M., Takeuchi, A., Awano, H., Niba, E. T. & Matsuo, M. Neuronal SH-SY5Y cells use the C-dystrophin promoter coupled with exon 78 skipping and display multiple patterns of alternative splicing including two intronic insertion events. *Hum. Genet.* **134**, 993–1001 (2015).
14 Gazzoli, I., Pulyakhina, I., Verwey, N. E., Ariyurek, Y., Laros, J. F., t Hoen, P. A. *et al.* Non-sequential and multi-step splicing of the dystrophin transcript. *RNA Biol.* **13**, 290–305 (2016).
15 Flanigan, K. M., Dunn, D. M., von Niederhausern, A., Soltanzadeh, P., Howard, M. T., Sampson, J. B. *et al.* Nonsense mutation-associated Becker muscular dystrophy: interplay between exon definition and splicing regulatory elements within the DMD gene. *Hum. Mutat.* **32**, 299–308 (2011).
16 Tran, V. K., Takeshima, Y., Zhang, Z., Yagi, M., Nishiyama, A., Habara, Y. *et al.* Splicing analysis disclosed a determinant single nucleotide for exon skipping caused by a novel intra-exonic four-nucleotide deletion in the dystrophin gene. *J. Med. Genet.* **43**, 924–930 (2006).
17 Magri, F., Del Bo, R., D'Angelo, M. G., Govoni, A., Ghezzi, S., Gandossini, S. *et al.* Clinical and molecular characterization of a cohort of patients with novel nucleotide alterations of the Dystrophin gene detected by direct sequencing. *BMC Med. Genet.* **12**, 37 (2011).
18 Wimmer, K., Roca, X., Beiglböck, H., Callens, T., Etzler, J., Rao, A. *et al.* Extensive *in silico* analysis of NF1 splicing defects uncovers determinants for splicing outcome upon 5' splice-site disruption. *Hum. Mutat.* **28**, 599–612 (2007).
19 Baralle, D. & Baralle, M. Splicing in action: assessing disease causing sequence changes. *J. Med. Genet.* **42**, 737–748 (2005).
20 Krawczak, M., Thomas, N. S. T., Hundrieser, B., Mort, M., Wittig, M., Hampe, J. *et al.* Single base-pair substitutions in exon-intron junctions of human genes: nature, distribution, and consequences for mRNA splicing. *Hum. Mutat.* **28**, 150–158 (2007).
21 ElSharawy, A., Hundrieser, B., Brosch, M., Wittig, M., Huse, K., Platzer, M. *et al.* Systematic evaluation of the effect of common SNPs on pre-mRNA splicing. *Hum. Mutat.* **30**, 625–632 (2009).
22 Takeshima, Y., Yagi, M., Wada, H., Ishibashi, K., Nishiyama, A., Kakumoto, M. *et al.* Intravenous infusion of an antisense oligonucleotide results in exon skipping in muscle dystrophin mRNA of Duchenne muscular dystrophy. *Pediatr. Res.* **59**, 690–694 (2006).
23 Lewandowska, M. A. The missing puzzle piece: splicing mutations. *Int. J. Clin. Exp. Pathol.* **6**, 2675–2682 (2013).
24 Gaildrat, P., Killian, A., Martins, A., Tournier, I., Frebourg, T. & Tosi, M. Use of splicing reporter minigene assay to evaluate the effect on splicing of unclassified genetic variants. *Methods Mol. Biol.* **653**, 249–257 (2010).
25 Takeshima, Y., Nishio, H., Sakamoto, H., Nakamura, H. & Matsuo, M. Modulation of *in vitro* splicing of the upstream intron by modifying an intra-exon sequence which is deleted from the dystrophin gene in dystrophin Kobe. *J. Clin. Invest.* **95**, 515–520 (1995).
26 Wang, Z., Lin, Y., Qiu, L., Zheng, D., Yan, A., Zeng, J. *et al.* Hybrid minigene splicing assay verified the pathogenicity of a novel splice site variant in the dystrophin gene of a Chinese patient with typical Duchenne muscular dystrophy phenotype. *Clin. Chem. Lab. Med.* **54**, 1435–1440 (2016).
27 Habara, Y., Takeshima, Y., Awano, H., Okizuka, Y., Zhang, Z., Saiki, K. *et al. In vitro* splicing analysis showed that availability of a cryptic splice site is not a determinant for alternative splicing patterns caused by +1G–>A mutations in introns of the dystrophin gene. *J. Med. Genet.* **46**, 542–547 (2009).
28 Habara, Y., Doshita, M., Hirozawa, S., Yokono, Y., Yagi, M., Takeshima, Y. *et al.* A strong exonic splicing enhancer in dystrophin exon 19 achieve proper splicing without an upstream polypyrimidine tract. *J. Biochem.* **143**, 303–310 (2008).
29 Nishida, A., Kataoka, N., Takeshima, Y., Yagi, M., Awano, H., Ota, M. *et al.* Chemical treatment enhances skipping of a mutated exon in the dystrophin gene. *Nat. Commun.* **2**, 308 (2011).
30 Desmet, F. O., Hamroun, D., Lalande, M., Collod-Beroud, G., Claustres, M. & Beroud, C. Human Splicing Finder: an online bioinformatics tool to predict splicing signals. *Nucleic Acids Res.* **37**, e67 (2009).
31 Yeo, G. & Burge, C. B. Maximum entrophy modeling of short sequence motifs with applications to RNA splicing signals. *J. Comput. Biol.* **11**, 377–394 (2003).
32 Sironi, M., Menozzi, G., Riva, L., Cagliani, R., Comi, G. P., Bresolin, N. *et al.* Silencer elements as possible inhibitors of pseudoexon splicing. *Nucleic Acids Res.* **32**, 1783–1791 (2004).
33 Wang, Y., Ma, M., Xiao, X. & Wang, Z. Intronic splicing enhancers, cognate splicing factors and context-dependent regulation rules. *Nat. Struct. Mol. Biol.* **19**, 1044–1052 (2012).
34 Flanigan, K. M., Dunn, D. M., von Niederhausern, A., Soltanzadeh, P., Gappmaier, E., Howard, M. T. *et al.* Mutational spectrum of DMD mutations in dystrophinopathy patients: application of modern diagnostic techniques to a large cohort. *Hum. Mutat.* **30**, 1657–1666 (2009).
35 Seo, S., Takayama, K., Uno, K., Ohi, K., Hashimoto, R., Nishizawa, D. *et al.* Functional analysis of deep intronic SNP rs13438494 in intron 24 of PCLO gene. *PLoS ONE* **8**, e76960 (2013).
36 Kashima, T., Rao, N. & Manley, J. L. An intronic element contributes to splicing repression in spinal muscular atrophy. *Proc. Natl Acad. Sci. USA* **104**, 3426–3431 (2007).
37 Thi Tran, H. T., Takeshima, Y., Surono, A., Yagi, M., Wada, H. & Matsuo, M. A G-to-A transition at the fifth position of intron 32 of the dystrophin gene inactivates a splice donor site both *in vivo* and *in vitro*. *Mol. Genet. Metab.* **85**, 213–219 (2005).
38 Deburgrave, N., Daoud, F., Llense, S., Barbot, J. C., Recan, D., Peccate, C. *et al.* Protein- and mRNA-based phenotype-genotype correlations in DMD/BMD with point mutations and molecular basis for BMD with nonsense and frameshift mutations in the DMD gene. *Hum. Mutat.* **28**, 183–195 (2007).
39 Aartsma-Rus, A., Fokkema, I., Verschuuren, J., Ginjaar, I., van Deutekom, J., van Ommen, G. J. *et al.* Theoretic applicability of antisense-mediated exon skipping for Duchenne muscular dystrophy mutations. *Hum. Mutat.* **30**, 293–299 (2009).
40 Matsuo, M., Takeshima, Y. & Nishio, H. Contributions of Japanese patients to development of antisense therapy for DMD. *Brain Dev.* **38**, 4–9 (2016).
41 Mendell, J. R., Goemans, N., Lowes, L. P., Alfano, L. N., Berry, K., Shao, J. *et al.* Longitudinal effect of eteplirsen versus historical control on ambulation in Duchenne muscular dystrophy. *Ann. Neurol.* **79**, 257–271 (2016).
42 Matsuo, M., Masumura, T., Nishio, H., Nakajima, T., Kitoh, Y., Takumi, T. *et al.* Exon skipping during splicing of dystrophin mRNA precursor due to an intraexon deletion in the dystrophin gene of Duchenne muscular dystrophy Kobe. *J. Clin. Invest.* **87**, 2127–2131 (1991).
43 Roest, P. A. M., Bout, M., van der Tuijn, A. C., Ginjaar, I. B., Bakker, E., Hogervorst, F. B. L. *et al.* Splicing mutations in DMD/BMD detected by RT-PCR/PTT: detection of a 19AA insertion in the cysteine rich domain of dystrophin compatible with BMD. *J. Med. Genet.* **33**, 935–9396 (1996).

Supplementary Information accompanies the paper on Journal of Human Genetics website (http://www.nature.com/jhg)